# Section Moment Capacity of a New Cold-formed Hollow Flange

Mahen Mahendran

Dhammika Mahaarachchi

Eighteenth International Specialty Conference on Cold-Formed Steel Structures
Orlando, Florida, U.S.A, October 26 & 27, 2006

# Section Moment Capacity of a New Cold-formed Hollow Flange Channel Section

Mahen Mahendran[1] and Dhammika Mahaarachchi[2]

## Abstract

Smorgon Steel Tube Mills has recently developed a new hollow flange channel section, named as LiteSteel Beam (LSB) using its patented dual electric resistance welding techniques. The new section is primarily intended for use as flexural members, targeting applications in the light industrial, commercial and domestic markets. Due to the unique shape and manufacturing process of the LiteSteel Beam section, section moment capacity and flexural behaviour are different to those experienced by the conventional plain channel sections. Therefore there is a need for test data on the section moment capacities of the new LSB sections. This paper describes a series of 16 section capacity tests of the new LiteSteel Beam sections. Four point bending tests were performed for 13 different LSB sections. The section moment capacities of LSB sections were compared with predictions from the current steel structures design standards. Based on the test results and comparisons, appropriate design recommendations have been proposed.

## 1. Introduction

The use of thin-walled, cold-formed high strength steel products in the building industry has significantly increased in recent years. These products are being widely used in various applications such as purlins, girts, portal frames and steel framed housing. With the availability of advanced roll-forming technologies and very thin (<1 mm) and high strength steels (>550MPa), cold-forming process has become simple, efficient and economical, capable of producing a variety of efficient sections including the rectangular and circular hollow sections. The hollow sections have a high torsional rigidity and thus give greater buckling strengths. Smorgon Steel Tube Mills (SSTM), a division of Smorgon Steel Group, first developed the so-called Dogbone sections or the Hollow Flange Beams (HFB) shown in Figure 1 using a dual electric resistance welding technology, for which it has worldwide patents. The structural efficiency of the HFB due to its torsionally rigid closed triangular flanges combined with an economical fabrication

[1]Professor, [2]Research Fellow, Queensland University of Technology, Brisbane, Queensland, Australia

process was the basis of HFB development (Dempsey, 1990). The HFBs combine the stability of hot-rolled steel sections with the high strength to weight ratio of conventional cold-formed steel sections, and thus are superior than the conventional sections. They have the hollow flanges away from the centre, making them more efficient flexural members than equivalent rectangular hollow sections. SSTM has recently improved the dual electric resistance welding and automated continuous roll-forming technologies and developed a new hollow flange section, the LiteSteel Beam (LSB) shown in Figure 2.

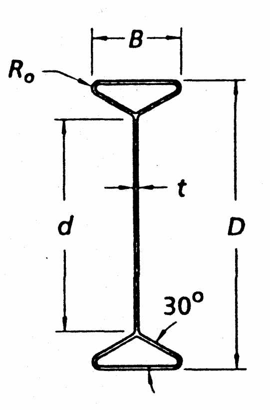


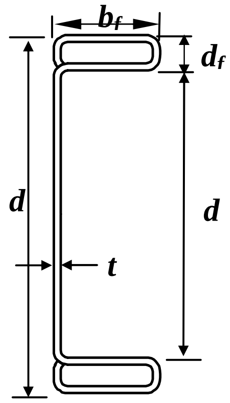


**Figure 1. Hollow Flange Beam (Dogbone)** **Figure 2. LiteSteel Beam**

The unique cold-forming and dual electric resistance welding process of LSB sections also introduces considerable differences in the stress-strain curves, residual stresses and initial geometric imperfections between them and the conventional hot-rolled and cold-rolled steel sections. The monosymmetric characteristics of the LSB are not present in the conventional I-section beams. Due to these reasons a comprehensive structural evaluation of LSB is therefore considered essential. Experimental data of conventional hot-rolled and cold-formed steel sections are inappropriate for use as the basis for the development of design rules of LSB sections. Therefore as the first step in this research on LSB sections an experimental investigation was conducted to study the flexural behaviour of LSB sections. Lateral distortional buckling and strength behaviour of LSB sections with medium and long lengths was investigated first and the details of this investigation and the results are given in another paper at this conference (Mahaarachchi and Mahendran, 2006).

Although the plastic bending strength and behaviour of conventional rectangular and square hollow sections have been extensively investigated (Hasan and Hancock, 1988 and Wilkinson, 1999), the results from these investigations are of limited use to LiteSteel Beam sections. The section capacity and plastic rotational capacity of the new LSB sections and the applicability of current steel design standards also have to be investigated. Therefore the LSB experimental investigation was extended to include short/fully laterally restrained LSB flexural members. A total of 16 LSB section capacity tests was undertaken in this investigation. Simply supported beams were tested to failure based on quarter point loading. This paper describes the section capacity tests of LSB sections, their results and comparisons with predictions from the current design rules.

## 2. Material and Section Properties

### 2.1 Material Properties

A series of tensile coupon tests was conducted for the batch of LSB sections from which the test beams were taken. Forty two tensile coupons were taken from the web and both inside and outside flanges of the LSB specimens and were tested according to the Australian Standard AS 1391 (SA, 1991). In order to determine the stress-strain relationship and the modulus of elasticity (E), two strain gauges were used on opposite sides of the coupons at their mid-height. Test results derived based on measured thicknesses are summarised in Table 1 while the typical stress-strain curves for the web and flanges are given in Figure 3. Test results show that the flange yield stress exceeds the nominal yield stress of 450 MPa and the web nominal yield stress of 380 MPa. As seen in Table 1, the average yield stresses of the outside and inside flanges and web were 516, 464 and 408 MPa, respectively, indicating the higher level of cold-working in the flanges. The lack of yield plateau in the stress-strain curves of flange specimens also demonstrates this (see Figure 3). The web and flange yield stresses varied depending on the thickness and LSB section.

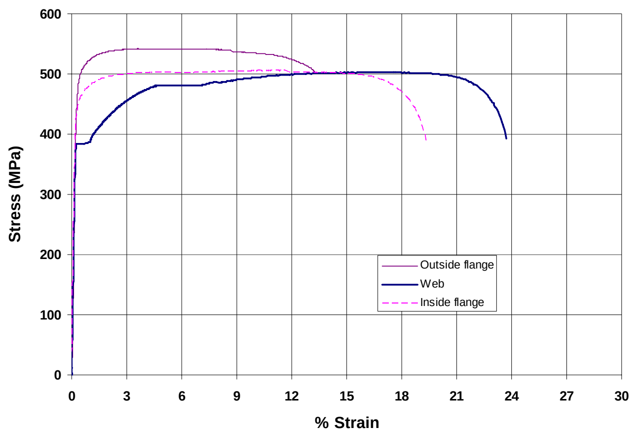


**Figure 3. Typical Stress-Strain Curves from Tensile Tests**

**Table 1. Tensile Test Results**

| Location | Yield stress (MPa) | Ultimate stress (MPa) | Young's Modulus (GPa) | 50 mm Elongation % |
|---|---|---|---|---|
| Outside Flange | 516 | 568 | 208 | 19.98 |
| Inside Flange | 464 | 523 | 206 | 26.78 |
| Web | 408 | 510 | 200 | 31.24 |

In addition to the determination of the yield stress and the Young's modulus, grid measurements were also used to evaluate the ductility parameters of total, local and uniform elongations. Clause 1.5.1.1 of AS/NZS 4600 (SA, 1996) recommends that the structural steel shall comply with one of the following standards: AS 1163 (SA, 1991), AS 1397 (SA, 2001), AS 1594 (SA, 2002), AS 1595 (SA, 1998) and AS/NZS 3678 (SA, 1996), as appropriate. Preliminary investigation at the University of Sydney (CASE, 2002) has shown that due to the unique manufacturing process used, LSB sections do not comply with the above standards. In such cases where clause 1.5.1.1 requirement is not met, AS/NZS 4600 (SA, 1996) allows their use provided Clause 1.5.1.5 requirements are met. According to Clause 1.5.1.5, steels not listed in Clause 1.5.1.1 and used for structural steel members and connections shall comply with one of the following requirements.

(a) The ratio of tensile strength to yield stress shall be not less than 1.08.

(b) The total elongation shall not be less than 10% for a 50 mm gauge length or 7% for a 200 mm gauge length standard specimen tested in accordance with AS 1391 (SA, 1991). If these requirements can not be met, the following criteria shall be satisfied.

- (i) Local elongation in a 13 mm gauge length across the fracture shall be not less than 20%.
- (ii) Uniform elongation outside the fracture shall be not less than 3%.

Tensile test results in Table 1 show that the average tensile strength to yield stress ratios of flanges and web were 1.10 and 1.25 (>1.08) respectively, while Figure 3 shows the minimum total elongation to be greater than 10%. Hence it can be considered that the steel used to manufacture the new LSB sections comply with the AS/NZS 4600 requirements.

## 2.2 Section Properties

The nominal section properties of LSB sections can be found in Dempsey (2001). They were calculated using an Excel spreadsheet program and nominal dimensions. The same program was used to calculate the actual section properties of test specimens used in this investigation. The measured thicknesses were found to be different to the nominal values. On average, the flanges were found to be thicker than the web by about 0.1 to 0.2 mm. A weighted average thickness was calculated for each section based on the flange and web areas and was then used in the Excel spreadsheet program to determine the accurate section properties of the specimens. Table 2 shows the nominal dimensions of the LSB sections used in this experimental investigation.

**Table 2. LSB Sections Used in Experiments**

| Test Section | Depth | Flange Width | Flange Depth | Thick-ness | Corner Radius | |
|---|---|---|---|---|---|---|
| | $d$ | $b_f$ | $d_f$ | $t$ | $r_o$ | $r_{iw}$ |
| | mm | mm | mm | mm | mm | mm |
| 300x75x3.0LSB | 300 | 75 | 25.0 | 3.00 | 4.50 | 3.00 |
| 300x75x2.5LSB | 300 | 75 | 25.0 | 2.50 | 3.75 | 3.00 |
| 300x60x2.0LSB | 300 | 60 | 20.0 | 2.00 | 3.00 | 3.00 |
| 250x75x3.0LSB | 250 | 75 | 25.0 | 3.00 | 4.50 | 3.00 |
| 250x75x2.5LSB | 250 | 75 | 25.0 | 2.50 | 3.75 | 3.00 |
| 250x60x2.0LSB | 250 | 60 | 20.0 | 2.00 | 3.00 | 3.00 |
| 200x60x2.5LSB | 200 | 60 | 20.0 | 2.50 | 3.75 | 3.00 |
| 200x60x2.0LSB | 200 | 60 | 20.0 | 2.00 | 3.00 | 3.00 |
| 200x45x1.6LSB | 200 | 45 | 15.0 | 1.60 | 2.40 | 3.00 |
| 150x45x2.0LSB | 150 | 45 | 15.0 | 2.00 | 3.00 | 3.00 |
| 150x45x1.6LSB | 150 | 45 | 15.0 | 1.60 | 2.40 | 3.00 |
| 125x45x2.0LSB | 125 | 45 | 15.0 | 2.00 | 3.00 | 3.00 |
| 125x45x1.6LSB | 125 | 45 | 15.0 | 1.60 | 2.40 | 3.00 |

## 2.3 Geometric Imperfections and Residual Stresses

The magnitudes of section and member imperfections were measured for each test specimen using both a Wild T05 theodolite and a new equipment based on a laser sensor. Measured values show that local plate imperfections are within the manufacturer's fabrication tolerance limits while overall member imperfections are less than span/1000.

Residual stress tests were conducted for three 150x45x1.6, two 250x75x2.5 and 300x75x3.0 LSB sections. The sectioning method was used to measure the longitudinal residual strains. Electrical strain gauges were used on both the inside and outside surfaces of the flanges to calculate the membrane and flexural residual stresses. The results showed that there are considerably large membrane stresses in the web due to the welding of the section. The measured residual strains were converted to residual stresses using a Young's modulus value of 200 GPa. They were then expressed as a ratio of the virgin plate's yield stress value of 380 MPa.

The LSB residual stresses were found to be both membrane and flexural stresses as shown in Figure 4 although conventional cold-formed steel sections have mainly flexural residual stresses. This is because LSB sections are manufactured using a combined cold-forming and welding process. Test results show that the magnitude of residual stress varied across the cross-section. The maximum flexural residual stress was recorded in the corner of the outside flange ($1.07f_y$) while that recorded in the web was $0.60f_y$, where $f_y$ is the virgin plate yield stress of 380 MPa.

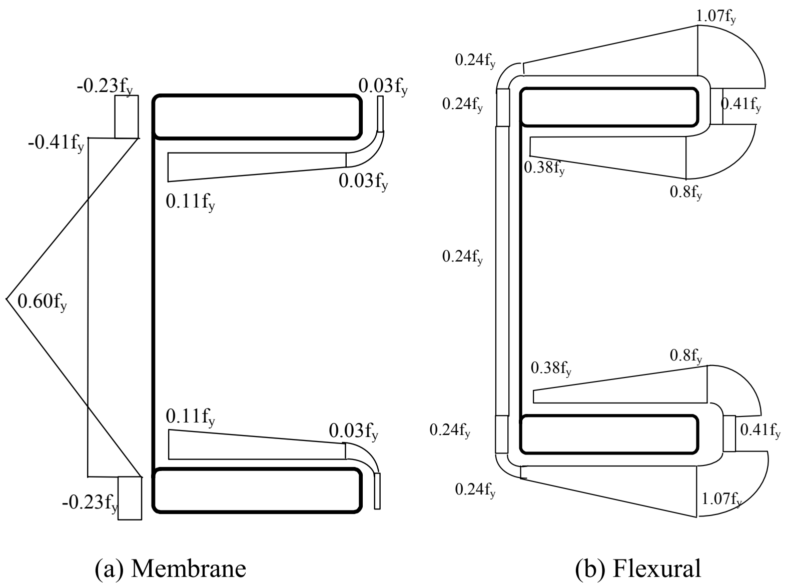


**Figure 4. Residual Stress Distribution in LSB Sections**

## 3. Section Capacity Tests of LiteSteel Beam Sections

### 3.1 Test Specimens

All the available LiteSteel Beam sections shown in Table 2 were selected in the test program so that the effects of the key parameters such as section geometry and the thickness and yield stress of steel could be investigated. This resulted in a total of 16 section capacity tests in this investigation (see Table 3).

### 3.2 Test Set-up and Procedure

The LSB section capacities were determined based on bending tests of a pair of LSB sections connected back to back with a 10 mm gap between them. This allowed the use of a symmetric and convenient test set-up and loading arrangement. The bending tests were undertaken using a 300 kN capacity

Tinious Olsen testing machine. Relatively short and fully laterally restrained LSB specimens were tested to failure using a four point bending test set-up. Figure 5 shows the section moment capacity test rig.

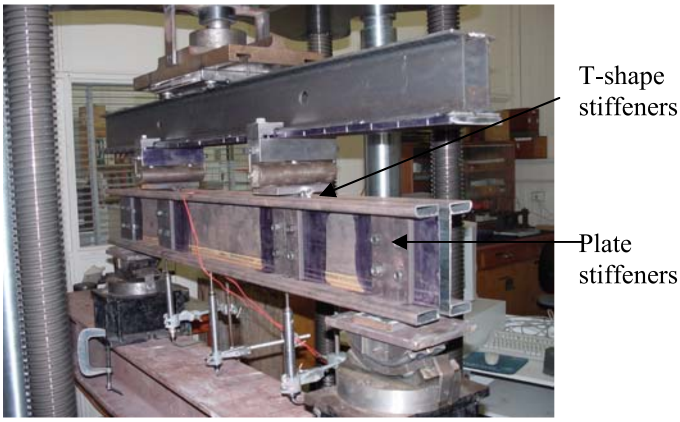


**Figure 5. Section Capacity Test Rig**

The simply supported beam specimens were tested by loading them symmetrically at two points on the span through a spreader beam that was loaded centrally by the ram of the testing machine. This four point bending arrangement provided a central region of uniform bending moment and zero shear force. The loading points on the test specimens were at a distance of span/3 from the end supports.

The load was applied to the top flange of LSB specimens through a steel roller placed on the top flange. The first test showed that the behaviour of the LSB sections was influenced by the high bearing stress imposed on the flanges as a result of the loading arrangement. The steel rollers caused a significant indentation on the flanges, leading to a premature failure of the section. In order to eliminate this problem T-shape and plate stiffeners were attached to either side of the webs of the beam specimens using four M10 bolts at both the loading and support points as shown in Figure 5. Applied loads were transferred to the beam webs through these stiffeners and hence could be considered to have been at the shear centre avoiding any eccentric loading and web crippling.

Although relatively short specimen lengths were chosen to avoid lateral buckling, some lateral movements were observed when the section started to yield, possibly due to the unsymmetrical nature of the back to back sections at this stage. This was avoided by providing lateral supports at 150 mm intervals to the compression flanges using an appropriate support system.

During the tests, the bending strains were measured using two strain gauges located on the top and bottom flanges of the specimen at midspan whereas the vertical beam deflections were measured using three displacement transducers located at midspan and loading points. The EDCAR data acquisition system was used to record all the strain and deflection data until the specimen failure. The cross head of the testing machine was moved at a constant rate of 1.0 mm/min until the specimen collapsed.

### 3.3 Test Results and Discussion

Applied maximum bending moment was calculated as the product of measured average applied load and the distance from the support to the loading point (span/3). The failure bending moment achieved by each test specimen and its failure mode are given in Table 3 whereas the typical moment-deflection/strain curves are shown in Figures 6 and 7.

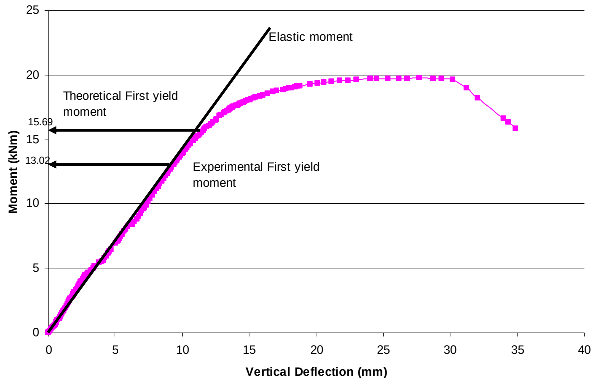


**Figure 6. Typical Moment vs Vertical Deflection of 150x45x2.0 LSB Sections**

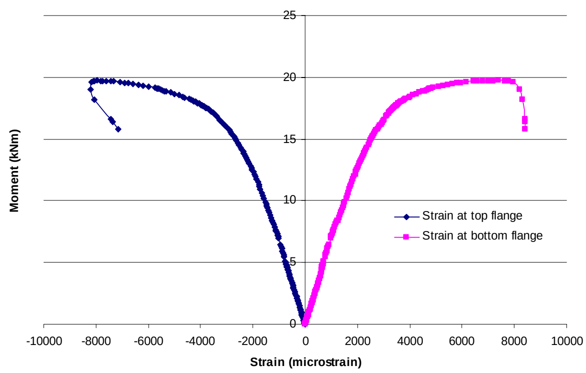


**Figure 7. Typical Moment vs Longitudinal Strain Variation of 150x45x2.0 LSB Sections**

All the specimens except the two 150x45x1.6 LSB sections (shear failure) experienced flange local buckling which produced a rapid unloading. When the top flange buckled, sympathetic rotation at the flange web corner caused deformation of the web. A typical local buckled specimen is shown in Figure 8. There was no sudden unloading associated with the lateral deflection and no specimen failed due to insufficient material ductility. Although failure modes after the tests appeared to be identical, there were some differences in the way the failure occurred. For compact LSB sections, large flange deformations and yielding occurred at moments closer to the failure moment and the moment-deflection curves had a long plateau. For non-compact sections, large flange deformations appeared to occur earlier and the plateau was reduced in length while for slender sections, local web buckling occurred which was followed by large flange deformations and yielding.

The moment-deflection/strain graphs in Figures 6 and 7 show that the initial response of the beams was linear. In theory, nonlinearity commences with the commencement of yielding, ie. at first yield moment. In practice yielding may be initiated before the ideal first yield point because of the high residual stresses present in the sections due to the cold-forming process used (Hasan and Hancock, 1988). Available results show that the first yield of LSB sections occurred at about 0.75 - 0.82 of theoretical first yield moment $M_y$.

**Figure 8. Typical Failures of Tested Specimens**

## 4. Comparison of Section Capacity with Current Design Methods

### 4.1 AS 4100 (SA, 1998)

The section moment capacity ($M_s$) is defined in AS 4100 Clause 5.2.1 (SA, 1998) as follows:

$$M_s = f_y Z_e \tag{1}$$

The effective section modulus ($Z_e$) allows for the effects of local buckling if necessary. The effective section modulus is defined in Clauses 5.2.3 to 5.2.5 (SA, 1998) as follows:

$$\lambda_s \le \lambda_{sp}: \quad Z_e = S < 1.5Z$$

$$\lambda_{sp} < \lambda_s \le \lambda_{sy}: \quad Z_e = Z + (S - Z)\left(\frac{\lambda_{sy} - \lambda_s}{\lambda_{sy} - \lambda_{sp}}\right) \qquad (2)$$

$$\lambda_s > \lambda_{sy}: \quad Z_e = Z\left(\frac{\lambda_{sy}}{\lambda_s}\right)$$

where S and Z are plastic and elastic section modulus, respectively

The section slenderness ($\lambda_s$) is taken as the value of the plate element slenderness ($\lambda_e$) for the element of the cross-section which has the greatest value of ($\lambda_e/\lambda_{ey}$). The plate element slenderness ($\lambda_e$) is defined in Clause 5.2.2 (SA, 1998) as a function of the element clear width (*b*), thickness (*t*), and yield stress ($f_y$).

$$\lambda_e = \frac{b}{t}\sqrt{\frac{f_y}{250}} \qquad (3)$$

The section plasticity and yield slenderness limits ($\lambda_{sp}$, $\lambda_{sy}$) are taken as the values of the element slenderness limits ($\lambda_{ep}$, $\lambda_{ey}$) given in Table 5.2 of AS 4100 (SA, 1998) for the element of the cross-section which has the greatest value of $\lambda_e/\lambda_{ey}$. The slenderness limit for cold-formed and lightly welded (CF/LW) elements was considered to be the most appropriate for LSB sections.

Note that both the measured web and flange yield stresses with the measured dimensions and the nominal web and flange yield stresses (380 MPa and 450 MPa, respectively) with the nominal dimensions were used to evaluate the plate element slenderness ratios using Equation 3, while the section yield stress in Equation 1 was taken as the flange yield stress. Section moment capacities based on these two methods are given in Table 3.

### 4.2 AS/NZS 4600 (SA, 1996)

The section moment capacity ($M_s$) is defined in Clause 3.3.2 of AS/NZS 4600 (SA, 1996) in a similar fashion to AS 4100 (see Equation 1). However, unlike AS 4100, the effective section modulus ($Z_e$) is based on the initiation of yielding in the extreme compression fibre and therefore does not allow for the inelastic reserve capacity of the section. The effects of local buckling are accounted for by using reduced widths ($b_e$) of non-compact elements in compression for the calculation of the effective section modulus (see Equation 4). Unlike AS 4100, the plate element slenderness is a function of the applied stress (f*), as shown in Equation 5. This accounts for the reduction in strength due to local buckling effects with increasing member slenderness.

$$b_e = \frac{1-0.22/\lambda}{\lambda} b \le b \tag{4}$$

$$\lambda = \frac{1.052}{\sqrt{k}}\left(\frac{b}{t}\right)\sqrt{\frac{f^*}{E}} \tag{5}$$

The section capacities of all LiteSteel Beam sections were calculated using the AS/NZS 4600 method described above, with local buckling coefficients (k) equal to 4 and 24 for the compression flange and web, respectively. Measured flange yield stress and section dimensions were used to calculate the section moment capacity and are given in Table 3.

**Table 3. Section Moment Capacity Results from Tests**

| LSB Specimen | Expt. Capacity (kNm) | Predicted Moment Capacity (kNm) | | Section compact | Exp./Pred. Ratio | |
|---|---|---|---|---|---|---|
| | | AS4600 | AS4100 | AS4100 | AS4600 | AS4100 |
| 150x45x1.6 | 15.23 Y | 12.77 | 13.42 | NC | 1.19 | 1.13 |
| 150x45x1.6 | 14.94 Y | 12.42 | 13.35 | NC | 1.20 | 1.12 |
| 150x45x2.0 | 19.63 Y | 15.69 | 16.90 | C | 1.25 | 1.16 |
| 125x45x2.0 | 14.38 Y | 12.14 | 13.20 | C | 1.18 | 1.09 |
| 125x45x1.6 | 12.95 Y | 9.90 | 11.32 | NC | 1.31 | 1.14 |
| 200x45x1.6 | 17.36 Y | 17.95 | 17.43 | S | 0.97 | 1.00 |
| 200x60x2.0 | 31.80 Y | 25.72 | 29.96 | NC | 1.24 | 1.06 |
| 200x60x2.5 | 52.47 Y | 33.89 | 41.87 | C | 1.55 | 1.25 |
| 250x60x2.0 | 47.33 LB/Y | 45.12 | 40.31 | S | 1.05 | 1.17 |
| 250x75x2.5 | 71.49 Y | 60.58 | 63.82 | C | 1.18 | 1.12 |
| 250x75x3.0 | 77.89 Y | 65.30 | 78.95 | C | 1.19 | 0.99 |
| 300x60x2.0 | 52.40 LB/Y | 57.65 | 41.48 | S | 0.91 | 1.26 |
| 300x75x2.5 | 85.80 | 77.34 | 69.61 | NC | 1.11 | 1.23 |
| 300x75x3.0 | 103.90 | 88.65 | 95.27 | NC | 1.17 | 1.09 |

Note: C=Compact, NC=Non-compact, S=Slender, Y=Yielding, LB=Local buckling

## 4.3 Discussion

As seen in Table 3, the experimental failure moments of all the test specimens exceeded the section moment capacities predicted by AS/NZS 4600 (SA, 1996) and AS 4100 (SA, 1998) except in two cases. On average AS/NZS 4600 underestimates the failure moment by 18% with a COV of 0.13 while AS 4100 predictions are 13% lower than the experimental moment capacity with a COV of 0.07. This comparison was made based on measured dimensions. From this comparison, it appears that AS/NZS 4600 predicts the section capacity of LSB sections more conservatively than AS 4100. This is because AS/NZS 4600 ignores the inelastic reserve capacity and considers only the first yield moment capacities and thus leads to conservative predictions for compact LSB sections (see high test to predicted ratios in Table 3). As observed in the tests, there was considerable moment capacity beyond the first yield point for such sections.

In contrast, the AS/NZS 4600 section capacity method more accurately estimates the reduction in capacity due to the local buckling effects in non-compact and slender sections, compared to the AS 4100 method. In general, AS/NZS 4600 prediction is conservative, and therefore it is safe to use the AS/NZS 4600 specifications for section capacity design checks of LSB sections subject to pure bending moment.

The high values of failure moment compared with predicted design capacities could be attributed to several factors, including strain hardening, the strength enhancement due to cold-forming especially in the flanges and the corners and residual stresses. The correlation between design standard predictions and experimental results was improved when measured properties are used.

## 5. Conclusions

This paper has presented the details of an experimental investigation of the section moment capacity of cold-formed and electric resistance welded LiteSteel Beam sections and the results. Four point bending tests were conducted for a total of 16 LitelSteel Beam sections. The test results are presented in the form of bending moment versus vertical deflection and longitudinal strains for each section. The maximum bending moment attained by each test specimen is listed and compared with design capacity predictions from the current steel design standards. LiteSteel Beam sections were found to have greater moment capacities than those predicted by the current steel design standards and therefore the current steel design standards can be used conservatively for the design of LiteSteel Beam sections. The cold-formed steel structures standard AS/NZS 4600 is more conservative in predicting the section moment capacity of compact LiteSteel Beam sections as it considers only the first yield moment.

## 6. References

CASE (2002), Further Advice on Project Genesis Sections, Investigation Report S 1346, Centre for Advanced Structural Engineering, University of Sydney, Sydney, Australia.

Dempsey, R.I. (1990), Structural Behaviour and Design of Hollow Flange Beams, Proc. of the Second National Structural Engineering Conference, Institution of Engineers, Australia, Adelaide, pp.327-335.

Dempsey, R.I. (2001), Hollow Flange Channel Development of the Product Range, Investigation Report, Warren Brown Associates, Brisbane, Australia.

Hasan, S.W and Hancock, G.J. (1988), Plastic Bending Tests of Cold-formed Rectangular Hollow Sections, Research report, The University of Sydney, Sydney, Australia.

Mahaarachchi, D. and Mahendran, M. (2006), Lateral Distortional buckling Behaviour of a New Cold-formed Hollow Flange Channel Section, Proc. of 18th International Specialty Conference on Cold-formed Steel structures, Orlando, Florida, USA

Standards Australia (SA) (1996), Cold-formed Steel Structures, AS/NZS 4600, Sydney, Australia.

Standards Australia (SA) (1991), Structural Steel Hollow Sections, AS 1163, Sydney, Australia.

Standards Australia (SA) (2001), Steel Sheet and Strip – Hot-dipped Zinc Coated or Aluminium/Zinc Coated, AS 1397, Sydney, Australia.

Standards Australia (SA) (2002), Hot-rolled Steel Flat Products, AS/NZS 1594, Sydney, Australia.

Standards Australia (SA) (1998), Cold-rolled, Unalloyed, Steel Sheet and Strip, AS/NZS 1595, Sydney, Australia.

Standards Australia (SA) (1996), Structural Steel – Hot-rolled Plates, Floor Plates and Slabs, AS/NZS 3678, Sydney, Australia.

Standards Australia (SA) (1998), Steel Structures, AS 4100, Sydney, Australia.

Standards Australia (SA) (1991), Methods for Tensile Testing of Metals, AS 1391, Sydney, Australia.

Wilkinson, T. (1999), The Plastic Behaviour of Cold-formed Rectangular Hollow Sections, PhD Thesis, The University of Sydney, Sydney, Australia.